

Embedded electronic system for evaluation of photovoltaic modules based on a current-voltage curve tracer

Ricardo Yauri^{1,2}, Rafael Espino¹

¹Facultad de Ingeniería, Universidad Tecnológica del Perú, Lima, Perú

²Facultad de Ingeniería, Universidad Privada del Norte, Lima, Perú

Article Info

Article history:

Received Sep 9, 2022

Revised Oct 18, 2022

Accepted Oct 24, 2022

Keywords:

Embedded system

I-V curve tracer

Microcontroller

Photocell

Portable device

Renewable energy

ABSTRACT

The rapid growth of the market for the use of renewable energy has increased the use of solar energy which has a significant role in power generation. This requires the insertion of equipment capable of providing precise measurements of the photovoltaic modules, either to verify the operation of the installation or to find specific problems. In this scenario, the current versus voltage curve tracer is used to describe the electrical behavior of the photovoltaic system through all the operating possibilities, but it has an excessive cost for small installations. This paper presents the development of a current-voltage curve tracer, capable of performing current, voltage and power measurements, contributing to the creation of equipment to test photovoltaic installations. The methods to obtain the I-V curves are presented and the characteristics of the embedded electronic system, which is based on an electronic load, are defined. As results, the simulations carried out for the variable load control, acquisition circuits and the implemented system are shown. In addition, the operation of the human-machine interface and the comparison with a commercial equipment are shown for reference.

This is an open access article under the [CC BY-SA](https://creativecommons.org/licenses/by-sa/4.0/) license.



Corresponding Author:

Ricardo Yauri

Facultad de Ingeniería, Universidad Tecnológica del Perú

125 Natalio Sanchez Road, Santa Beatriz, Lima, Perú

Email: boncer99@gmail.com

1. INTRODUCTION

Electric power is considered a basic need of modern society due to its usefulness for sustainable economic development. As a result of the use of fossil energy sources, there were serious negative environmental impacts, such as carbon dioxide (CO₂) emissions, global warming, air pollution, deforestation and environmental degradation. As the price of conventional energy rises, new, clean alternatives have begun to emerge and become increasingly competitive [1]. Due to favorable conditions, both in terms of solar resource and political climate, a substantial increase in solar photovoltaic capacity was also observed in several Latin American and Caribbean countries [2].

Many countries have a growing interest in producing electricity on a small scale characterized by the use of small power generators connected to the electrical system and located in the vicinity of the places of consumption [3]. In this case, photovoltaic sources are the best to adapt, since it is possible to install these systems on the roofs of houses, shopping centers, companies or other buildings, with a low environmental impact [4], [5]. The number of modules used in a photovoltaic system depends on its generation capacity. In the process of assembling photovoltaic systems, to avoid damaging them, it is necessary to carry out a visual inspection, start-up tests, performance evaluation and subsequent periodic maintenance of the photovoltaic system (mainly in the case of large or complex installations) [6], [7].

Photovoltaic systems go through performance tests related to irradiance values and temperature, which are carried out under certain climatic conditions so as not to affect current and voltage measurements [8], [9]. Such a requirement creates obstacles in the start-up process, since the adequate conditions are only reached in hours close to noon and due to clouds, the irradiance incident on the modules can vary very quickly [10], [11]. Due to this, it is essential to use specialized measurement equipment, which provides reliable results, streamlining verification procedures and allowing immediate identification of problems in the installation and operation [12], [13].

Currently, there is a variety of specialized commercial equipment known as "I-V curve tracer" (current-voltage curve tracer), which are capable of providing the most complete information possible on a photovoltaic system [14], since they reveal what is happening with a photovoltaic source, in addition to presenting quantitative measurements and a qualitative visual representation of your performance [15]. These do not allow modifications to expand their operating characteristics, so there is a tendency to build them based on a heterogeneous set of hardware and software technologies [16]. Non-commercial tracers are based on hardware devices such as microcontroller (MCU) ATmega2560 [17], [18], ATMEGA328 [19], Atmel SAM3X8E [20], MSP430 [21], TivaC [22], PIC18F46K22 [23], and Raspberry PI [16], which are used for validation of laboratory prototypes, automation of measurement and visualization processes [18] using, in most cases, devices with low hardware resources [24]. In addition, some solutions perform the presentation of the results, trace curves, using standard computer equipment, databases [16], [18], [19], data analysis software such as MATLAB [21], Labview [22] and Python [19], [16], without considering local monitoring capabilities such as liquid-crystal display (LCD) touch screens [23]. In addition to this, validations of the systems are carried out only with simulation [25] or using synthetics [19], [20], therefore the mentioned limitations can be reduced by adding wireless transmission capabilities [26], granting mobility to the device and contributing to reduce the gap in your research with solutions based on portable and ubiquitous systems.

This paper describes the development of an I-V curve tracer, detailing its main characteristics, the method chosen, based on a variable electronic load and the implementation process. Therefore, a study of the characteristics of a photovoltaic module and the factors that can change its operation was carried out. The paper continues with section 2, where the characteristics of an I-V curve tracer are shown. Section 3 presents the characteristics of the built embedded electronic device. It continues with section 4 where the insulated gate bipolar transistor (IGBT) device is evaluated as a variable load. Finally, section 5 presents the results of the operation of the I-V curve tracing equipment and the conclusions in section 6.

2. I-V CURVE TRACER

The use of loads that are not constant allows to analyze the points in which the sources operate that allow drawing the graphs that relate the current and voltage (curve I-V). This is achieved by varying the current between the values corresponding to the short circuit (ISC) and open circuit values (VOC) [27], [28]. The procedure described above is usually conducted with this variable load that can be found in special equipment, which also has analog signal acquisition, data processing and control stages. It is important to consider that among the most important sensors there are solar irradiation and temperature sensors as shown in Figure 1. This type of equipment has voltage measurement ranges that could reach up to 1,500 volts [29].

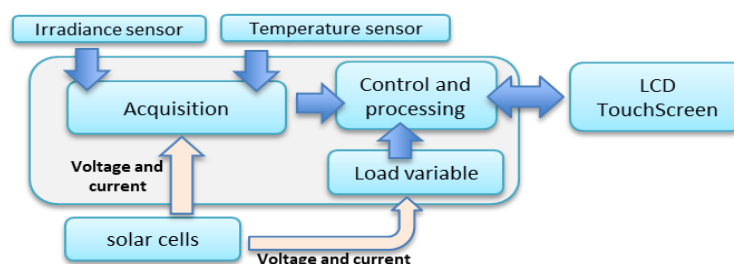


Figure 1. General diagram of an I-V curve tracer

2.1. Methods to obtain the characteristic curves

The research papers describe procedures to obtain the parameters that describe the behavior of the current/voltage relationship (I-V Curves) and power/voltage (power and voltage curves). The investigations do not coincide in the way of taking the data through the sampling process. The selection of the type of load to use it in a control equipment [21], [22], [25]. Among the different characterization methods, we have:

- Variable resistive load. Under controlled conditions they are used to evaluate solar cells, where a set of resistances can be considered to form these curves.
- DC-DC converter with resistive load. To generate a change in current, the output power is varied, which also modifies voltage values.
- Electronic load. Semiconductor-based transistor devices generate current by injecting voltage into their terminals. Devices such as IGBTs can usually be used [30].
- Capacitive load. It allows to obtain a relationship between the capacitance and the stabilization time through its transient analysis where the energy source is the photovoltaic cell.

3. SYSTEM CHARACTERISTICS

3.1. Typical characteristics

Using the load electronics method is the most appropriate according to the characteristics considered for the I-V curve tracer system and this is due to the need to build a device that can move to different environments and has a reduced implementation cost. In addition, an IGBT device was added because it is necessary to consider high values in voltage MOSFETs and an embedded electronic system is developed to conduct the process of drawing curves through variable load, which uses analog signal acquisition blocks and control stages. A graphical user interface is added to obtain and enter signals related to solar irradiance and the number of photovoltaic modules connected in series and other of the acquired parameters corresponds to the temperature of the photovoltaic module. The scheme of the entire system is shown in Figure 2.

The use of an LCD touch screen has been considered to observe the generated curves and is controlled by the STM32F746NG microcontroller and available pins are added for connection with another circuit (the acquisition circuit and the variable load circuit) and external secure digital (SD) memories. To acquire the voltage signal, it is necessary to use an arrangement of resistors to adapt the signal level, which is complemented by an operational amplifier. A voltage signal is generated, controlled by the microcontroller, through a digital/analog converter (DAC) which enters the IGBT device allowing control of the variable load, forming the control circuit of the embedded electronic system. Finally, this system also has a Wi-Fi module, which allows wireless communication with another device capable of performing irradiance and temperature measurements in addition to communicating with a computer. The system has a maximum cost of 180 dollars by integrating the SMT32F (\$56), IGBT (\$19), acquisition circuit (\$70) and other components (cables, fans and heat sink) which makes it cost less than other equipment. professionals that integrate more functionalities than necessary.

3.2. IGBT characteristics

The IGBT selected for this development was the IXYH82N120C3, being a high-speed device. The most important parameter is the maximum power at which the load is capable of dissipating, limiting the electrical characteristics of the equipment. Therefore, the acquisition circuit does not need to cover the entire range of voltage and current.

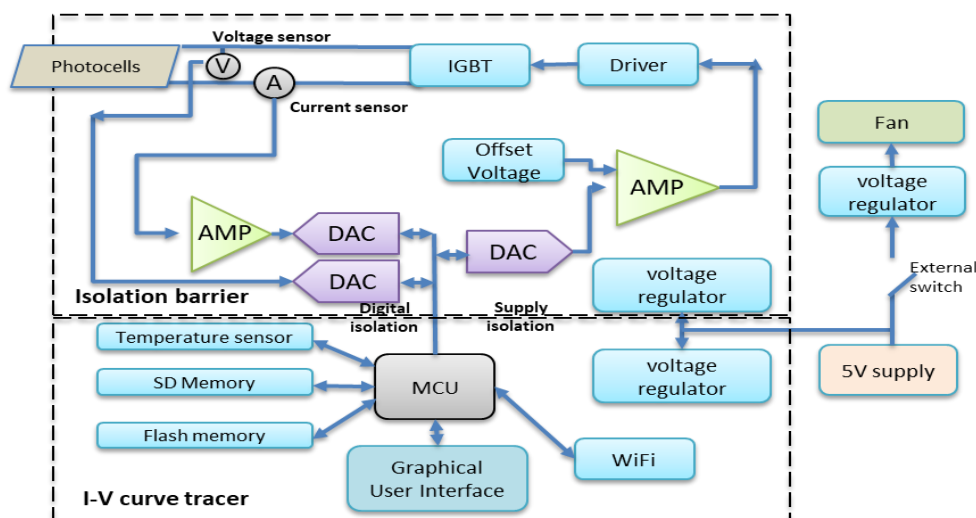


Figure 2. Schematic of developed I-V curve tracer

Based on the electrical characteristics of the selected IGBT and the measurement ranges, voltage and current of the acquisition circuit considered for this development. It was proposed that the equipment have the electrical characteristics shown in Table 1.

Table 1. Electrical characteristics of the embedded electronic system

	Range	Resolution	Precision
Voltage	2 - 600 V	0,1	1 %
Current	0,01 - 10 A	0,01	1 %
Power	2 - 1000 W	1	1 %

4. EVALUATION OF IGBT AS VARIABLE LOAD

Figure 3 shows a photovoltaic source based on the CS6K-270P module which is connected to an IGBT module. Circuit simulation is performed using a PSpice model of the IGBT (model IXYN82N120C3) and the variation from the IGBTV threshold voltage of 3 V to 7 V is considered. In this case the voltage value on the resistor between the IGBT emitter and collector is low enough to generate a short circuit. The largest variation of the photovoltaic module voltage occurs for a reduced voltage range of the control signal, especially between the voltages $V_{GE} = 5 \text{ V}$ and $V_{GE} = 5.4 \text{ V}$ of the IGBT. Therefore, the currents and voltages obtained allowed selecting the control voltage values shown in Table 2.

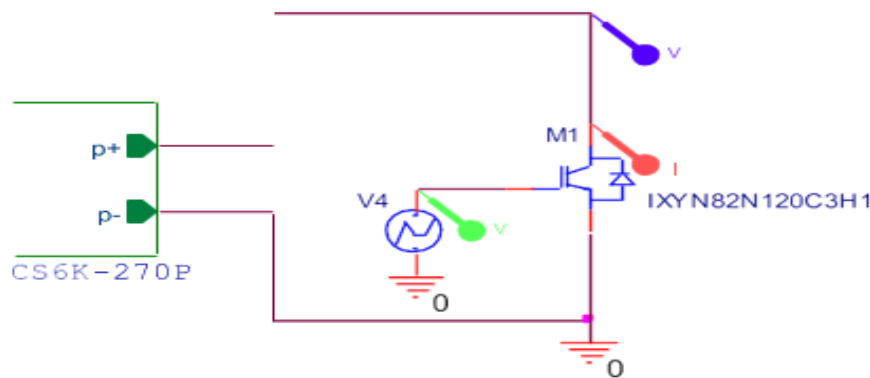


Figure 3. Diagram of an IGBT as an electronic load applying a control signal

Table 2. Voltages applied to the IGBT gate

V_{ge} (V)	Voltage (V)	Current (A)
3	37,64	0
4,9	36,92	1,62
5	36,33	2,86
5,1	35,49	4,41
5,2	34,24	6,28
5,25	33,28	7,34
5,3	31,61	8,46
5,33	27,88	9,17
5,333	25,13	9,25
5,334	20,25	9,27
5,335	9,9	9,29
5,34	1,75	9,31
7	1,22	9,31

Due to the characteristics of the module, it is necessary to obtain an amplified signal between 0 and 4 V at the IGBT gate, requiring an amplifier gain (G) of around 1.21 V/V. To satisfy these requirements, the use of the AD5621A DAC, with 12 bits of resolution, and the THS4031 operational amplifier in a non-inverting summing amplifier configuration are considered. Furthermore, since the control signal at the IGBT gate must be proportional to the DAC ramp signal, it is convenient to use the ZXTC2063E6 controller, which consists of a combination of NPN and PNP transistors as shown in Figure 4 [31].

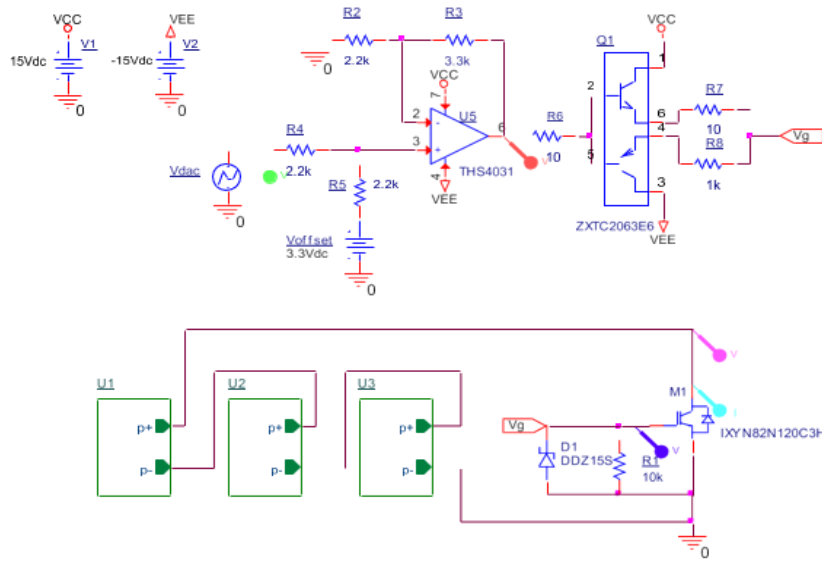


Figure 4. DAC signal conditioning circuit and driver for IGBT control, connected with an array of three photovoltaic modules

5. RESULTS

5.1. System hardware construction

Schematic diagrams and printed boards of the electrical circuits involved in the prototype of the embedded electronic system were designed. The section that corresponds to the DAC module is shown in Figure 5. In addition, the offset voltage circuit is observed, with a fixed output at 3.3 V, the control signal conditioning circuit and the IGBT. The acquisition of current and voltage signals is highlighted using the MAX11100 ADC.

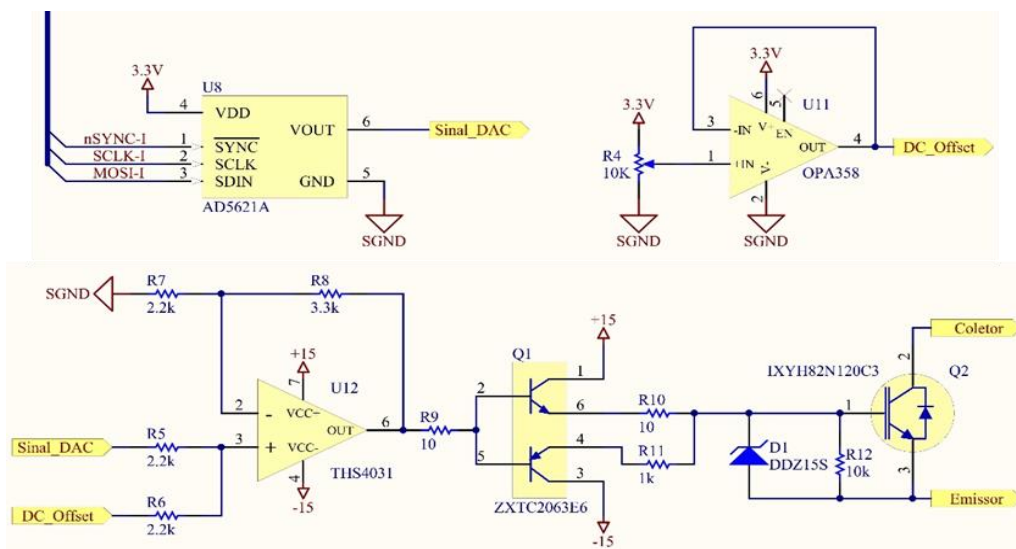


Figure 5. Schematic circuit diagram for IGBT control

It is necessary to carry out a construction process that implies the implementation of a printed circuit board and protection structure as shown in Figure 6. The printed circuits were implemented considering the restrictions of available space and power, obtaining as a result the power printed circuit shown in Figure 6(a). Once the components were available, they were integrated and fixed in a PVC box, which allowed the equipment to be portable as shown in Figure 6(b). Furthermore, the power circuit is electrically isolated from the user using the structure and the IGBT, the heat sink, the fan, power supply circuit and the temperature sensor can be seen in Figure 6(b).

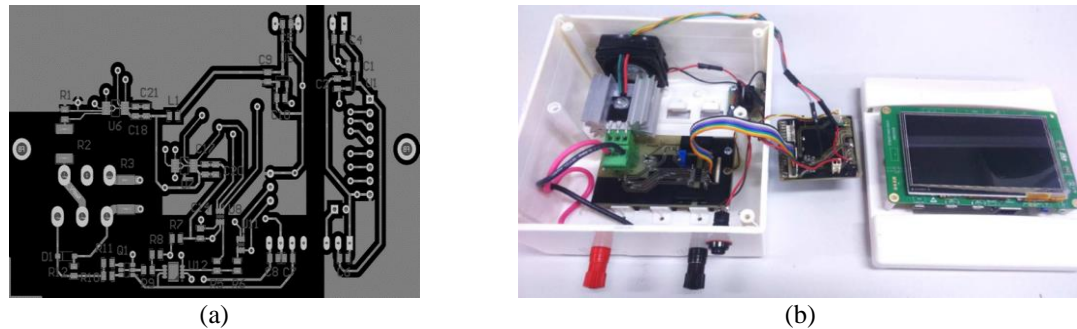


Figure 6. Implementation of the system considering (a) the view of the power printed circuit board and (b) the internal part of the developed system

5.2. System implementation

The operation of this system is based on a state machine, which starts from an initial state and changes when it is necessary to finish the execution of a function, or an option is selected through the user interface. The system implements a main function called “Initial Configuration” which performs the configuration of the system clock, the timer, internal modules of the MCU, the SD and FLASH memory, LCD screen and touch interface which is part of the graphical user interface. The equipment has functions called “Show I-V Curve” and “Show P-V Curve” whose operation is shown in Figure 7.

The discovery development module was used for the development of the system, which integrates the 32-bit STM32F746NG microcontroller (from the STMicroelectronics company) and a 4.3” LCD-TFT color screen with touch interface. This LCD screen is configured by means of an LTDC module (LCD-TFT display controller) using the SPI communication protocol (serial peripheral interface using 4 wires) to send and receive data to the microcontroller. In addition, the software used to trace the signal on the screen is implemented directly in C language (without the use of external design libraries or frameworks) directly manipulating the pixels from the microcontroller due to the simplicity of the signals to be displayed. On the other hand, the developed software needs to detect the presence of a photovoltaic source between its terminals, to carry out the previously explained tracing processes by means of a state machine.

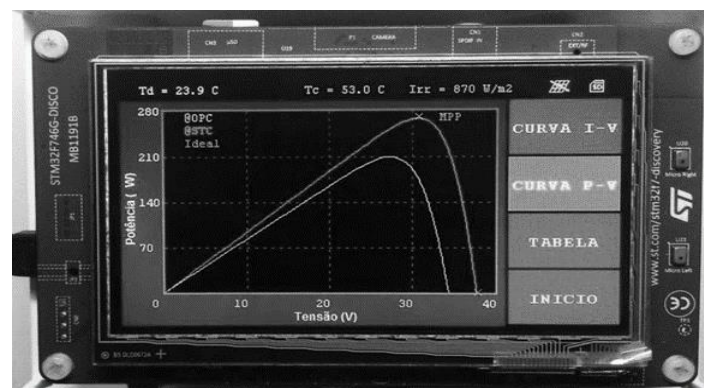


Figure 7. Presentation of the P-V curves in a graphical user interface

5.3. Functional and calibration tests

Tests are performed to evaluate and validate each designed and implemented subcircuit, considering the variable load using an oscilloscope to visualize the signals as shown in Figure 8. The configurations made by the microcontroller are validated, verifying that it can control the different devices connected to it (the LCD, the DAC and the external ADCs) as shown in Figure 8(a). Using a Tektronix DPO 3,014 oscilloscope, the signal is obtained at the DAC output, at the amplifier and at the IGBT gate. The time required for the data acquisition function to be completed is 492 ms, which is enough so that the external environmental conditions do not have significant variations during the procedure. Figure 8(b) shows the oscilloscope screen where the acquisition time and the control signal are observed.

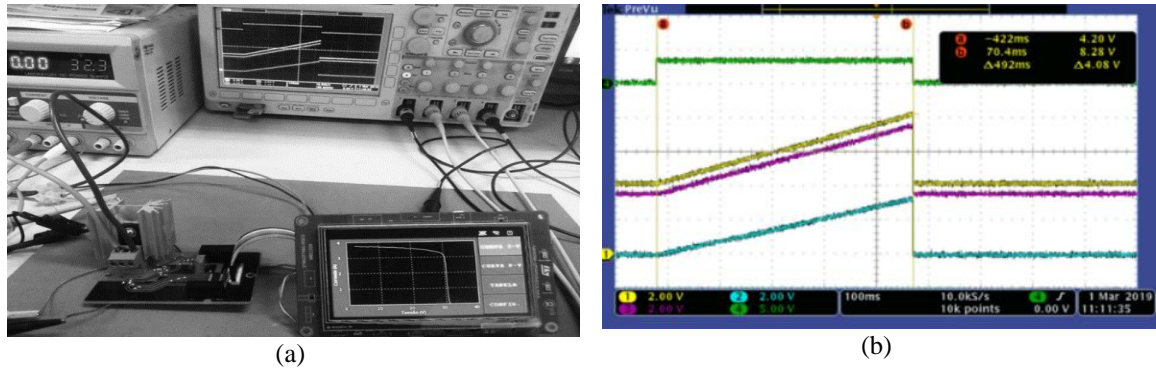


Figure 8. System tests for (a) verify the designed circuits and acquisition algorithms and (b) test to obtain the time that the control signal takes from the minimum value to the maximum value

5.4. Field tests with photovoltaic array

The behavior of the system with a photovoltaic module in external environments is evaluated, initially considering the comparison with commercial equipment. The results about the conditions of temperature and irradiance acquired with the two devices are presented in Table 3. While Figure 9 shows the I-V and P-V curves generated by each device. It is possible to observe the similarity of the compared curves, the adjustment for losses carried out in the tests being unnecessary.

Table 3. Electrical parameters acquired by the system under operating conditions

Variable	Proposed system	Solar I-Ve
Temperature (°C)	50	51
Irradiance (W/m2)	812	797
Pmax (W)	141,04	133.14
Vmp (V)	32.95	32.30
Imp (A)	4.28	4.12
Voc (V)	41.21	40.75
ISc (A)	4.68	4.44

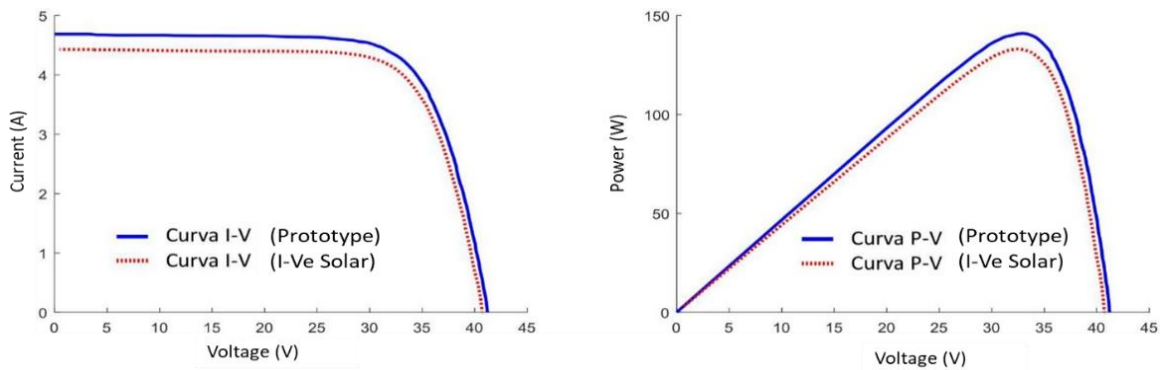


Figure 9. I-V and P-V characteristic curves of the developed equipment (blue) and of the commercial equipment (red)

6. CONCLUSION

From the results shown, it can be concluded that the developed system provides a representation of the behavior of solar photocells by tracing I-V curves in a functional and comparable way to a commercial equipment, highlighting the use of a human-machine interface through the touch screen. The characteristics of the embedded electronic system are defined and validated through its implementation, previously performing the simulation of the variable load control through the IGBT device. The curve tracer system in this paper can be improved by integrating machine learning algorithms to add predictive features about I-V curve status and generate web monitoring applications for remote tracking.

ACKNOWLEDGEMENTS

Thanks to the University of Campinas (UNICAMP) and the National Council for Scientific and Technological Development (CNPq) for their support during the development of the paper.

REFERENCES

- [1] R. Foster, M. Ghassemi, and A. Cota, "Introduction to Solar Energy," CRC Press, 2020, doi: 10.1201/9781420075670-8/INTRODUCTION-SOLAR-ENERGY.
- [2] R. Now, "Renewables 2019 global status report," *Renewable Energy Policy Network for the 21st Century*, 2019. [Online]. Available: http://www.ren21.net/Portals/97/documents/GSR/REN21_GSR2011.pdf
- [3] P. Megantoro, P. Anugrah, Y. Afif, L. J. Awalim, and P. Vigneshwaran, "A practical method to design the solar photovoltaic system applied on residential building in Indonesia," *Indones. J. Electr. Eng. Comput. Sci.*, vol. 23, no. 3, pp. 1736–1747, Sep. 2021, doi: 10.11591/IJEECS.V23.I3.PP1736-1747.
- [4] N. S. Ma'aji, H. Adun, A. Shefik, M. Adedeji, and M. Dagbasi, "Design of trigeneration plant for electricity freshwater production, and district heating: A case study periwinkle lifestyle estate, Lagos Nigeria," *Case Stud. Therm. Eng.*, vol. 35, Jul. 2022, doi: 10.1016/J.CSITE.2022.102041.
- [5] R. Kuwahara, H. Kim, and H. Sato, "Evaluation of zero-energy building and use of renewable energy in renovated buildings: A case study in Japan," *Buildings*, vol. 12, no. 5, May 2022, doi: 10.3390/BUILDINGS12050561.
- [6] D. J. Sambor, M. Wilber, E. Whitney, and M. Z. Jacobson, "Development of a tool for optimizing solar and battery storage for container farming in a remote arctic microgrid," *Energies*, vol. 13, no. 19, Oct. 2020, doi: 10.3390/EN13195143.
- [7] V. B. Pamshetti, S. Singh, and S. P. Singh, "Reduction of energy demand via conservation voltage reduction considering network reconfiguration and soft open point," *Int. Trans. Electr. Energy Syst.*, vol. 30, no. 1, Jan. 2020, doi: 10.1002/2050-7038.12147.
- [8] A. A. Stephen, K. Musasa, and I. E. Davidson, "Modelling of solar PV under varying condition with an improved incremental conductance and integral regulator," *Energies*, vol. 15, no. 7, Apr. 2022, doi: 10.3390/EN15072405.
- [9] I. M. Kirpichnikova, K. Sudhakar, I. B. Makhsumov, A. S. Martyanov, and S. S. Priya, "Thermal model of a photovoltaic module with heat-protective film," *Case Stud. Therm. Eng.*, vol. 30, Feb. 2022, doi: 10.1016/J.CSITE.2021.101744.
- [10] K. Ali *et al.*, "Robust integral backstepping based nonlinear MPPT control for a PV system," *Energies*, vol. 12, no. 16, Aug. 2019, doi: 10.3390/EN12163180.
- [11] A. Asbayou, A. Aamoume, M. Elyaqouti, A. Ihlal, and L. Bouhouch, "Benchmarking study between capacitive and electronic load technic to track I-V and P-V of a solar panel," *Int. J. Electr. Comput. Eng.*, vol. 12, no. 1, pp. 102–113, Feb. 2022, doi: 10.11591/IJECE.V12I1.PP102-113.
- [12] D. N. Karamov and K. V. Suslov, "Storage battery operation in autonomous photovoltaic systems in Siberia and the Russian Far East. Practical operating experience," *Energy Reports*, vol. 8, pp. 649–655, Apr. 2022, doi: 10.1016/J.EGYR.2021.11.184.
- [13] X. F. Wu, C. Y. Yang, W. Ch. Han, and Z. R. Pan, "Integrated design of solar photovoltaic power generation technology and building construction based on the internet of things," *Alexandria Eng. J.*, vol. 61, no. 4, pp. 2775–2786, Apr. 2022, doi: 10.1016/J.AEJ.2021.08.003.
- [14] H. B. Chi, M. F. N. Tajuddin, N. H. Ghazali, A. bin Azmi, and M. U. Maaz, "Internet of things (IoT) based i-v curve tracer for photovoltaic monitoring systems," *Indones. J. Electr. Eng. Comput. Sci.*, vol. 13, no. 3, pp. 1022–1030, Mar. 2019, doi: 10.11591/IJEECS.V13.I3.PP1022-1030.
- [15] P. Gevorkian, *Large-scale solar power system design: an engineering guide for grid-connected solar power generation*. McGraw-Hill Education, 2011. Accessed: Aug. 29, 2022. [Online]. Available: <https://www.accessengineeringlibrary.com/content/book/9780071763271>
- [16] I. González, J. M. Portalo, and A. J. Calderón, "Configurable IoT open-source hardware and software I-V curve tracer for photovoltaic generators," *Sensors 2021, Vol. 21, Page 7650*, vol. 21, no. 22, p. 7650, Nov. 2021, doi: 10.3390/S21227650.
- [17] A. Rivai, N. A. Rahim, M. F. M. Elias, and J. Jamaludin, "Multi-channel photovoltaic current-voltage (I-V) curve tracer employing adaptive-sampling-rate method," *IET Sci. Meas. Technol.*, vol. 14, no. 8, pp. 969–976, Oct. 2020, doi: 10.1049/IET-SMT.2019.0338.
- [18] S. R. Davronov, "Autonomous multifunctional measuring device for monitoring the characteristics of photovoltaic modules," *Appl. Sol. Energy (English Transl. Geliotekhnika)*, vol. 56, no. 2, pp. 118–124, Mar. 2020, doi: 10.3103/S0003701X2002005X.
- [19] H. M. Aguilar and K. J. M. Peña, "Low cost automatic I-V curve generator for solar cells," *Phys. Educ.*, vol. 54, no. 5, 2019, doi: 10.1088/1361-6552/AB2568.
- [20] A. Boucharef, A. Tahri, F. Tahri, S. Silvestre, and M. Bourahla, "Solar module emulator based on a low-cost microcontroller," *Meas. J. Int. Meas. Confed.*, vol. 187, Jan. 2022, doi: 10.1016/J.MEASUREMENT.2021.110275.
- [21] Z. Chen, Y. Lin, L. Wu, S. Cheng, and P. Lin, "Development of a capacitor charging based quick I-V curve tracer with automatic parameter extraction for photovoltaic arrays," *Energy Convers. Manag.*, vol. 226, 2020, doi: 10.1016/J.ENCONMAN.2020.113521.
- [22] M. Cáceres *et al.*, "Low-Cost I-V tracer for PV modules under real operating conditions," *Energies*, vol. 13, no. 17, Sep. 2020, doi: 10.3390/EN13174320.
- [23] S. B. Pal, A. Das, K. Das, and D. Mukherjee, "Design of a low-cost measuring and plotting device for photovoltaic modules," *Meas. Control (United Kingdom)*, vol. 52, no. 9–10, pp. 1308–1318, Nov. 2019, doi: 10.1177/0020294019865752.
- [24] R. Yauri, J. Lezama, and M. Rios, "Evaluation of a wireless low-energy mote with fuzzy algorithms and neural networks for remote environmental monitoring," *Indones. J. Electr. Eng. Comput. Sci.*, vol. 23, no. 2, pp. 717–724, Aug. 2021, doi: 10.11591/IJEECS.V23.I2.PP717-724.
- [25] V. Kongphet, A. Migan-Dubois, C. Delpha, J. Y. Lechenadec, and D. Diallo, "Low-Cost I-V tracer for PV fault diagnosis using single-diode model parameters and I-V curve characteristics," *Energies*, vol. 15, no. 15, Aug. 2022, doi: 10.3390/EN15155350.
- [26] R. Yauri, A. Castro, R. Espino, and S. Gamarra, "Implementation of a sensor node for monitoring and classification of physiological signals in an edge computing system," *Indones. J. Electr. Eng. Comput. Sci.*, vol. 28, no. 1, pp. 98–105, Oct. 2022, doi: 10.11591/IJEECS.V28.I1.PP98-105.
- [27] M. Jaber, A. S. A. Hamid, K. Sopian, A. Fazlizan, and A. Ibrahim, "Prediction model for the performance of different PV modules using artificial neural networks," *Appl. Sci.*, vol. 12, no. 7, Apr. 2022, doi: 10.3390/APP12073349.
- [28] M. K. Basher, M. Nur-E-alam, M. M. Rahman, S. Hinckley, and K. Alameh, "Design, development, and characterization of highly efficient colored photovoltaic module for sustainable buildings applications," *Sustain.*, vol. 14, no. 7, Apr. 2022, doi: 10.3390/SU14074278.

- [29] H. T. Instruments, "I-V500w I-V curve tracer and IVCK tester up to 15A or 1500VDC," 2021. Accessed: Aug. 28, 2022. [Online]. Available: www.ht-instruments.com
- [30] O. Alavi, L. V. Cappellen, W. De Ceuninck, and M. Daenen, "Practical challenges of high-power igt's I-V curve measurement and its importance in reliability analysis," *Electron.*, vol. 10, no. 17, Sep. 2021, doi: 10.3390/ELECTRONICS10172095.
- [31] D. O. Brunner *et al.*, "Symmetrically biased T/R switches for NMR and MRI with microsecond dead time," *J. Magn. Reson.*, vol. 263, pp. 147–155, Feb. 2016, doi: 10.1016/J.JMR.2015.12.016.

BIOGRAPHIES OF AUTHORS



Ricardo Yauri    is a Master of Science in Electronic Engineering with a Mention in Biomedical. He is associate professor at the Universidad Nacional Mayor de San Marcos (UNMSM) and PhD student in Systems Engineering. He is professor at Universidad Tecnológica del Perú and Universidad Peruana del Norte. He has participated as a teacher in courses oriented to the Internet of things and applications in home automation and the Cisco academy for IoT. He was researcher at INICTEL-UNI in the embedded systems and internet of things research group. He developed research projects on the implementation of low consumption IoT devices that involve inference techniques, machine learning algorithms and computational intelligence. He can be contacted at boncer99@gmail.com, c24068@utp.edu.pe, ryaurir@unmsm.edu.pe.



Rafael Espino    is specialist in the development of electronic systems with solid knowledge in photovoltaic systems and extensive experience in implementing embedded firmware in electronic systems. He is a graduate of the Faculty of Electronics of the National University of Engineering. He is currently a professor at the Universidad Tecnológica del Perú and at the Universidad de Ingeniería y Tecnología. With aptitudes for teaching, research and project management. He can be contacted at rafalloelo@gmail.com.